160

The Stress-Optic Effect in Optical Fibers

ARTHUR J. BARLOW AND DAVID N. PAYNE

Abstract—**The importance of the photoelastic effect in controlling polarization in optical fibers is discussed. Measurements of the stress-optic coefficient, its dispersion, and temperature dependence are reported using a fiber measurement method. The results compare closely to data obtained for bulk silica by an extrapolation technique. It is shown that the dispersion of the stress-optic coefficient can have a significant effect on the performance of birefringent fibers and of fiber birefringent devices. Furthermore, the temperature dependence is sufficiently large to be troublesome in fiber sensors.**

I. Introduction

THE photoelastic (or stress-optic) effect forms the basis of a number of methods for controlling the polarization properties of single-mode optical fibers. For example, a large stress anisotropy can be induced in a fiber which has an asymmetric cross section by using materials which differ greatly in expansion coefficient [1], [2]. As a result of the stress-optic effect, the fiber will have high optical birefringence. Consequently, its polarization properties will not be significantly affected by external perturbations (bends, twists, pressure) which themselves induce a similar, but very much smaller, photoelastic birefringence. The two birefringent axes are therefore stable, and the fiber is able to transmit a single linear polarization state aligned with one of these axes.

A similar principle can be used to transmit circularly polarized light by introducing a large circular-birefringence (optical rotation) [3], [4]. To achieve this, the fiber is tightly twisted, and the torsional stresses induce a photoelastic rotation of the plane of polarization. Provided the circular birefringence is sufficiently large compared to the externally induced birefringence, the fiber will conserve a single circularly-polarized mode. Both linear and circular polarization-maintaining fibers are useful in interferometric sensors [5], and may also be employed in phase-coherent telecommunications links [6] where the output polarization state is important.

Further exploitation of the photoelastic effect may be found in a class of devices which make use of birefringent fibers [7] or of controlled bending birefringence [8]. Distributed fiber versions of discrete retarders and rotators have been made and used to control polarization state [9]. Wavelength-selective filters [10] have also been demonstrated, as have a number of pressure-selective transducers [11], [12].

Despite the widespread use of the photoelastic effect in fibers, surprisingly little is known of the value in the infrared of the stress-optic coefficient C for silica and doped-silica fiber materials or of its variation with wavelength and temperature. The wavelength dispersion of C is important when operating devices which depend on the photoelastic effect over a range of wavelengths as, for example, in wavelength-multiplexed systems. It can also lead to errors in measurements of the wavelength dependence of fiber birefringence where it is common to assume that the stress-induced refractive-index anisotropy is independent of wavelength.

In addition, the dispersion in C contributes to the fiber pulse dispersion [13]. The variation of C with temperature, on the other hand, reduces the stability of fiber birefringent devices and can considerably affect the operation of fiber sensors.

The object of this work is to measure the wavelength and temperature dependence of the stress-optic coefficient in doped-silica fibers over the wavelength range 1–1.6 μm and compare the results to those obtained for bulk silica. We show that the value of $dC/d\lambda$ differs only slightly from that of silica, and is essentially constant over the range of wavelengths normally of interest. It is thus relatively easy to incorporate the effect into calculations of birefringence and mode dispersion. We also show that the variation of C with temperature is sufficiently large to be troublesome in a number of potential applications.

II. Stress-Optic Coefficient in Bulk Silica

Values for the stress-optic coefficient of silica in the infrared and its wavelength dispersion are not directly available. However, it has previously been recognized that the dispersion of the photoelastic effect in silica and other glasses follows essentially the same law as that for the birefringence of crystal quartz for which extensive data have been published [14]. It is thus possible to normalize the known silica stress-optic coefficient $C(\lambda_0)$ at wavelength λ_0 to the birefringence of quartz at the same wavelength, and use the established dispersion equation for crystal quartz to predict the stress-optic coefficient $C(\lambda)$ as a function of wavelength λ [14]:

$$\frac{C(\lambda)}{n_s(\lambda)} = C(\lambda_0)\left[\frac{n_s(\lambda_0)}{n_s^2(\lambda)} \cdot \frac{\lambda^2}{\lambda_0^2} \cdot \frac{\lambda_0^2 - \lambda_1^2}{\lambda^2 - \lambda_1^2} \cdot \frac{\lambda^2 - \lambda_2^2}{\lambda_0^2 - \lambda_2^2}\right] \quad (1)$$

where

$n_s(\lambda)$ = refractive index at wavelength λ
λ_0 = normalizing wavelength
λ_1 = 0.1215 μm
λ_2 = 6.900 μm.

The derivative of (1) with respect to wavelength gives the dispersion in the stress-optic coefficient $dC/d\lambda$. The results for $C(\lambda)$ and $dC/d\lambda$ are shown in Figs. 1 and 2, respectively,

Manuscript received April 19, 1982. This work was supported in part by a Fellowship from the Pirelli General Cable Company to D. N. Payne and in part by the U.K. Science and Engineering Research Council and the Central Electricity Research Laboratories.

The authors are with the Department of Electronics, University of Southampton, SO9 5NH, Hampshire, England.

0018-9197/83/0500-0834$01.00

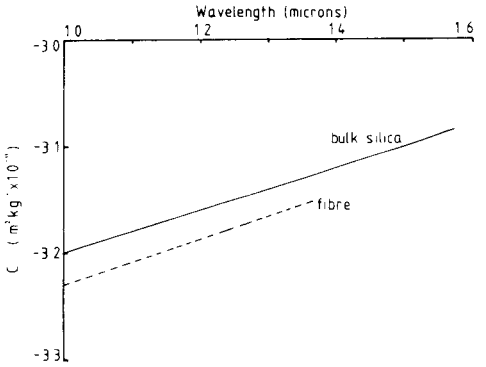

Fig. 1. Variation of stress-optic coefficient C with wavelength. Solid line is result extrapolated for bulk silica and dashed line is that measured for a GeO_2-doped fiber.

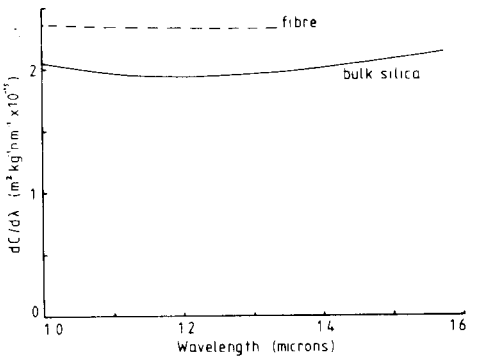

Fig. 2. Comparison of the dispersion in the stress-optic coefficient ($dC/d\lambda$) for bulk silica (solid line) and GeO_2-doped fiber (dashed line).

where we have used the data of Malitson [15] for the values of $n_s(\lambda)$ and $dn_s/d\lambda$ in bulk silica. C is taken as -3.30×10^{-11} $m^2 \cdot kg^{-1}$ at $\lambda_0 = 0.633$ μm [16]. It can be seen that C varies relatively slowly, and that $dC/d\lambda$ is essentially constant at a value of $\sim 2.0 \times 10^{-15}$ $m^2 \cdot kg^{-1} \cdot nm^{-1}$ over the wavelength range of 1.0–1.6 μm.

III. Stress-Optic Coefficient in a Doped-Silica Fiber

A. Measurement Techniques

There are a number of ways in which the stress-optic coefficient can be measured as a function of wavelength in a fiber. For example, the variation of fiber stress birefringence with wavelength could be used, provided the intrinsic birefringence can be associated solely with the photoelastic effect. In practice, the measurement is complicated by the presence of both a waveguide-shape birefringence component B_G and a thermal stress component B_S [13], as well as a potential externally induced birefringence due to handling the fiber. In addition, there exists a strong variation of birefringence with temperature, caused primarily by changes in the expansion coefficients of the fiber constituent materials. It is therefore an advantage to altogether eliminate from the measurements the effects of fiber linear birefringence.

In a spun fiber [13], [17], the intrinsic birefringence is made negligibly small by averaging the phase index of the two orthogonally polarized fiber modes [18]. The fiber is twisted during drawing, while the glass is in a molten state so that a permanent twist is frozen into the structure. The effect is to produce a fiber with virtually no measurable birefringence or optical rotation and, moreover, no observable change of birefringence with temperature. The fiber, therefore, has no polarization effects of its own, and is ideal for the purpose of measuring the stress-optic coefficient. We can now externally add a controlled stress-induced birefringence in one of two ways: 1) by bending [19] and 2) by twisting the fiber [3]. Bending a fiber requires winding under tension on a former, which leads to radial pressure and additional undesirable birefringence. We have therefore chosen twisting as being simpler and more accurate.

B. Experiment

When a fiber is twisted, an elastooptic rotation of the plane of polarization α occurs, given by [3]

$$\alpha = g'\xi = \frac{-RC\xi}{n_c}. \tag{2}$$

Here g' is the stress-optic rotation coefficient, ξ is the applied twist rate, n_c is the core refractive index, and R is the modulus of rigidity. In general, α, g', C, and n_c are functions of wavelength. The dispersion of the stress-optic coefficient $dC/d\lambda$ is obtained from (2) as

$$\frac{dC}{d\lambda} = -\frac{1}{R}\left[g'\frac{dn_c}{d\lambda} + n_c(\lambda)\frac{dg'}{d\lambda}\right]. \tag{3}$$

Thus, provided $n_c(\lambda)$ and $dn_c/d\lambda$ are known for the core glass, a measurement of g' as a function of wavelength gives C and $dC/d\lambda$.

The measurement of the wavelength variation of twist-induced rotation was performed on an uncoated 0.9 cm pitch spun fiber [17] which had a silica core doped with 3.4 m/o GeO_2 and a depressed B_2O_3/SiO_2 cladding within a silica substrate of 73 μm OD. The cutoff wavelength was 0.95 μm and the core/cladding index difference was $\sim$0.5 percent, of which 0.27 percent was due to the GeO_2-doped core. The fiber was hung vertically to prevent bends and to ensure a uniform twist in the 1.3 m length. Both ends were anchored with minimal introduction of stress by using silicone rubber adhesive, and five turns of twist were applied. The wavelength-tunable source was the Raman output from a single-mode fiber pumped with a Q-switched Nd:Yag laser [20]. The twist-induced rotation was measured using a polarizer and analyzer.

The results obtained for the stress-optic rotation coefficient g' are shown in Fig. 3 (dots), together with a fitted second-order Chebyshev curve (dashed). For comparison, the expected variation of g' for bulk silica is plotted as a solid line, calculated from (1) and (2). For the latter, we have used the data of Malitson for $n_s(\lambda)$ and $R = 3.19 \times 10^9$ $kg \cdot m^{-2}$ [16] in (2). It can be seen that g' varies almost identically in the doped fiber and in bulk silica, with the fiber value being slightly higher ($\sim$5 percent) and more dispersive.

Reference to (2) and (3) shows that to compute C and $dC/d\lambda$ from the experimental data of Fig. 3, we require $n_c(\lambda)$ and $dn_c/d\lambda$ for the doped-glass core. Although these values can be computed directly from previously published data on GeO_2-

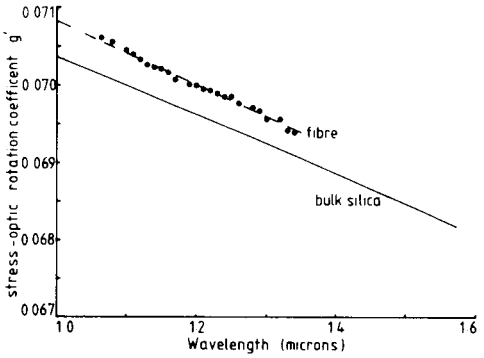

Fig. 3. Variation of the stress-optic rotation coefficient g' with wavelength. Points are experimental values with fitted line (dashed). Solid line is value computed from data for bulk silica.

doped fibers [21], calculations show that for the small index difference in the fiber (0.27 percent) due to GeO_2, the values of $dn_c/d\lambda$ and $n_c(\lambda)$ differ by less than ~1 percent from those of silica (see the Appendix). The use of silica values [15] therefore produces a negligible error in C and $dC/d\lambda$ and will be used here.

The results for C and $dC/d\lambda$ in the fiber computed from the experimental data of Fig. 3 are shown overlayed on those for bulk silica in Figs. 1 and 2, respectively. Referring to Fig. 1, we see that the value of C is very slightly higher in the fiber than that extrapolated for bulk silica. Our measured fiber value C (1.3 μm) = -3.17×10^{-11} m$^2 \cdot$ kg^{-1} also agrees well with that found for a fiber in [22] ($C = -3.36 \times 10^{-11}$ m$^2 \cdot$ kg^{-1}). It is remarkable that the agreement between fibers and bulk silica should be so close in view of the disparity between reported values for C in the literature [23]. Moreover, the fiber samples contain GeO_2, and we may therefore infer that its presence in small quantities does not significantly affect the stress-optic coefficient.

Reference to Fig. 2 reveals that $dC/d\lambda$ is also very similar in our fiber and in bulk silica, the fiber value being ~10 percent higher. The variation in the curve for silica also closely resembles that for the fiber, and this tends to confirm the dispersive law adopted for C in (1).

The variation of the stress-optic coefficient with wavelength has implications when measuring fiber polarization properties as a function of wavelength. For example, the fiber beat length $L_p = \lambda/B_S$ will still appear to vary approximately linearly with wavelength since $dC/d\lambda$ is small and nearly constant, but the slope of the variation will differ by between 6 and 10 percent from that expected.

IV. Polarization Mode Dispersion

Asymmetric radial stress in a "single-mode" fiber leads to the existence of two orthogonally polarized modes aligned with the axes of stress asymmetry. As a result of the stress-optic effect, the two modes have different phase and group velocities (polarization mode dispersion [24]). The dispersion in the stress-optic coefficient will modify the group-delay difference between modes, and thus contribute to the polarization mode dispersion.

A. Linearly Birefringent Fibers

In general, the fiber will exhibit a waveguide birefringence B_G due to an asymmetry in the waveguiding structure, as well as a stress-optic birefringence B_S. For a linearly birefringent fiber with a difference $\delta\beta$ in mode propagation constants, the group-delay difference $\Delta\tau_0$ between modes is [13]

$$\Delta\tau_0 = \frac{L}{c}\frac{d(\delta\beta)}{dk} = \frac{L}{c}\frac{d}{dk}[k(B_G + B_S)]$$

$$= \frac{L}{c}\left[B_G + k\frac{dB_G}{dk} + B_S\left(1 + \frac{k}{c}\frac{dC}{dk}\right)\right] \quad (4)$$

where L is the fiber length and c is the velocity of light. The final term in (4) represents the contribution due to the stress-optic coefficient. Evaluation of $k/C \cdot dC/dk$ using the results of Figs. 1 and 2 yields a value of 9.5×10^{-2} at a 1.3 μm wavelength, i.e., the stress-optic effect increases the polarization mode dispersion due to stress by 9.5 percent. For many purposes, it may therefore normally be neglected. We note in passing that, in addition to the intermode dispersion discussed here, the dispersion in C will contribute to the total chromatic dispersion of each mode. However, in this case, it is the second derivative $d^2C/d\lambda^2$ which is important. As $dC/d\lambda$ is approximately constant with wavelength (Fig. 2), calculations show the contribution to be negligible ($<10^{-15}$ s $\cdot$ nm^{-1} $\cdot$ km^{-1}) compared to material and waveguide chromatic dispersion, even in very highly stressed, polarization-maintaining fibers.

B. Circularly Birefringent Fibers

When a fiber is highly twisted at a rate ξ, the intrinsic linear birefringence tends to be quenched by the large twist-induced circular birefringence [3], [18]. The fiber then supports two approximately circularly polarized modes with opposite rotations and with a difference in propagation constants $\delta\beta_{circ} = 2g'\xi$. Such a fiber has been proposed as a circular polarization-maintaining fiber [4]. The polarization mode dispersion $\Delta\tau_c$ is given by

$$\Delta\tau_c = \frac{L}{c}\frac{d}{dk}(\delta\beta_{circ}) = \frac{2L}{c}\xi\frac{dg'}{dk}. \quad (5)$$

In this case, the residual polarization mode dispersion is due solely to the dispersion in the stress-optic coefficient.

The value of $\Delta\tau_c$ is plotted as a function of wavelength in Fig. 4 for a fiber having a twist of 50 turns/m, using the data of Fig. 3. The curve is given both for the measured fiber results and for bulk silica. A dispersion of 2.2 ps/km is found for the fiber at $\lambda = 1.3$ μm. This is close to the value expected for a nominally circular telecommunications-grade fiber, which typically has a small linear stress birefringence. Moreover, it is probable that higher twists than 50 turns/m will be required to maintain a given circularly polarized mode [25], thus increasing the dispersion.

V. Temperature Dependence of the Photoelastic Effect

A. Measurement

The measurement of the variation of the photoelastic constant with temperature was performed on the same spun fiber with applied twist. As before, a spun fiber exhibits no birefringence or temperature effects of its own and, is ideal for the purpose.

The temperature dependence of C can be obtained from g' in (2) and its derivative with respect to temperature T:

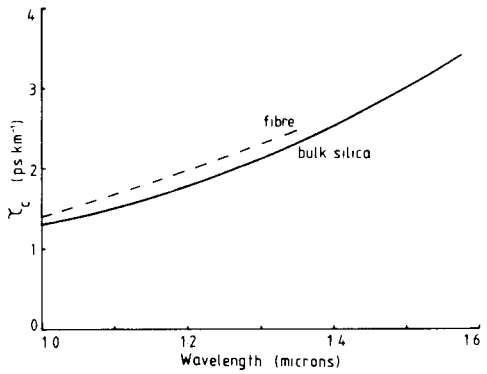

Fig. 4. Calculated polarization mode dispersion in a fiber twisted at 50 turns/m as a function of wavelength. Dashed line is computed for fiber, solid line for bulk silica.

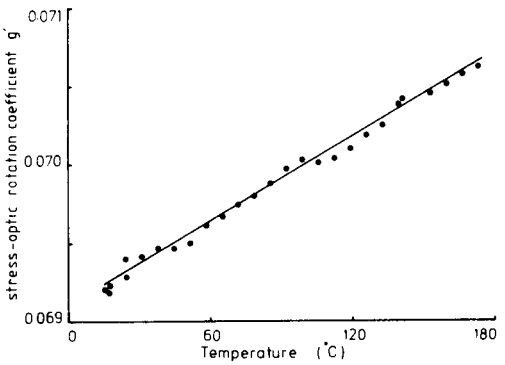

Fig. 5. Variation of stress-optic rotation coefficient g' with temperature at 1.064 μm wavelength.

$$\frac{dC}{dT} = -\frac{1}{R}\left[g' \frac{dn_c}{dT} + n_c(T)\frac{dg'}{dT}\right]. \quad (6)$$

Thus, provided $n_c(T)$ and dn_c/dT are known, a measurement of g' as a function of temperature gives C and dC/dT.

The variation of twist-induced optical rotation was determined at a wavelength of 1.06 μm on the same length of fiber as in the previous experiment. The fiber was hung vertically within a 1 m long tube furnace and five turns of twist were applied. The measured variation of g' is shown in Fig. 5 over the temperature range 20–180°C, together with a first-order Chebyshev fit. The stress-optic rotation coefficient is seen to vary linearly with temperature over the full temperature range, with a slope dg'/dT of 8.95×10^{-6} K^{-1}. This gives a temperature coefficient $1/g' \cdot dg'/dT$ of 1.27×10^{-2} percent · K^{-1}, which compares well to the value of 0.96×10^{-2} percent · K^{-1} reported previously on a very similar fiber [26].

As previously justified, we will use the values of bulk silica for $n_c(T)$ and dn_c/dT in (6) to determine dC/dT. The variation of index with temperature dn_s/dT has been measured [15] as 10.93×10^{-6} K^{-1} at $T = 25$°C and $\lambda = 1.064$ μm. From (6), we therefore obtain $dC/dT = -4.31 \times 10^{-15}$ m^2 · kg^{-1} · K^{-1} at $T = 25$°C and $\lambda = 1.064$ μm. We have been unable to find a previous reference to the measured value of dC/dT for bulk silica for comparison. However, [27] gives $dC/dT \sim -3.34 \times 10^{-15}$ m^2 · kg^{-1} · K^{-1} for a high silica glass with composition 67.5 percent SiO_2, 15.4 percent B_2O_3, 16.7 percent K_2O, and 0.4 percent MgO. Our result indicates that silica and lightly doped silica behave similarly.

B. Effect of Temperature on Birefringent Fiber Devices

Bending Birefrinence: Controlled bending birefringence $\delta\beta_B$ is used to fabricate fiber isolators [8], polarization controllers [9], and wavelength filters [10]. For a fiber with radius r bent with a radius of curvature R, $\delta\beta_B$ is given by [19]

$$\delta\beta_B = \frac{\pi EC}{\lambda}\left(\frac{r}{R}\right)^2 \quad (7)$$

where $E = 7.45 \times 10^9$ kg · m^{-2} [16] is Young's modulus. The fractional change in bend birefringence is

$$\frac{d}{dT}(\delta\beta_B) \cdot \frac{1}{\delta\beta_B} = \left(1/C \frac{dC}{dT} + \frac{1}{E}\frac{dE}{dT}\right). \quad (8)$$

Evaluation of (8) at 1.064 μm using $dE/dT = 1.03 \times 10^6$ kg · m^{-2} · K^{-1} [28] gives 0.027 percent · K^{-1}, which is considerably less than the value of 0.063 percent · K^{-1} reported for a similar fiber in [26] at a wavelength of 0.633 μm. Recently, further measurements have been made in our laboratory [29] directly on a bent fiber, using a 40-turn formerless coil [8]. These results were obtained at 0.633 μm and give a fractional change in bend birefringence of 0.01–0.02 percent · K^{-1}, thus tending to confirm the present findings.

A Faraday-effect optical isolator can be constructed from a small coil of fiber using the principle of exactly matching the phase beat length due to bending birefringence to the coil circumference over some 40 turns [8]. The temperature variation of bending birefringence will produce a mismatch in the coil, and the Faraday rotation will be consequently reduced. Using the measured temperature coefficient, we calculate that the degree of isolation will be degraded to 25 dB for a temperature change of ±10°C.

The temperature coefficient of bend birefringence will similarly affect the performance of all fiber devices based on controlled bending birefringence. Fortunately, the effect is not large and can normally be accounted for.

The temperature variation of fiber beat length in a linearly birefringent fiber is also affected by the change in C. Calculations and experiments in our laboratory indicate that in a fiber dominated by anisotropic thermal stress, the birefringence varies by ~0.1 percent · K^{-1}. Similar considerations to those above for bend birefringence indicate that the variation in C contributes about 15 percent to the observed temperature dependence of the fiber beat length.

Twist: Twisting is commonly used to assuage the effects of the linear birefringence which is inevitably present in the fiber. For example, a twisted fiber Faraday-effect current transducer has been constructed [30], and it was noted that the output polarization state was temperature dependent, giving a zero drift. Using the temperature coefficient of g' measured here, we see that a 20 m coil of fiber twisted at a rate of 20 turns/m would have an output plane of polarization which would vary by 1.3 K^{-1}.

The use of twisted fibers has been considered in a number of applications, such as in coherent optical transmission or in fiber interferometers. Although twisting the fiber will certainly reduce the temperature dependence of the intrinsic linear birefringence due to thermal stress, it is worth noting that a residual variation of the twist-induced birefringence remains.

TABLE I
SUMMARY OF STRESS-OPTIC PARAMETERS MEASURED FOR SILICA FIBER DOPED WITH 3.4 m/o GeO_2

Parameter	Symbol	Units	Value at 1.064μm	Value at 1.3μm
Stress-optic coefficient	C	$m^2\ kg^{-1}$	-3.22×10^{-11}	-3.17×10^{-11}
Wavelength dispersion in C	$dC/d\lambda$	$m^2\ kg^{-1} nm^{-1}$	2.34×10^{-15}	2.32×10^{-15}
Relative dispersion in C	$1/C.\ dC/d\lambda$	$\%\ nm^{-1}$	-0.00729	-0.00734
Temperature coefficient of C	dC/dT	$m^2\ kg^{-1}\ K^{-1}$	-4.31×10^{-15}	-
Relative temp. coefficient of C	$1/C\ dC/dT$	$\%\ K^{-1}$	0.0134	-
Stress-optic rotation coefficient	g'	-	0.0706	0.0696
Wavelength dispersion in g'	$dg'/d\lambda$	nm^{-1}	-4.56×10^{-6}	-4.56×10^{-6}
Relative dispersion in g'	$1/g'.\ dg'/d\lambda$	$\%\ nm^{-1}$	-0.0065	-0.0066
Temperature coefficient of g'	dg'/dT	K^{-1}	8.95×10^{-6}	-
Relative temp. coefficient of g'	$1/g'.\ dg'/dT$	$\%\ K^{-1}$	0.0127	-

VI. CONCLUSIONS

By performing measurements on a twisted fiber, we have quantified the variation of the stress-optic coefficient with wavelength and temperature in a GeO_2-doped fiber. Comparison to the extrapolated results for bulk silica shows close agreement, suggesting that: 1) light doping of silica, and 2) the thermal history do not significantly affect its photoelastic properties. The key results for the variation of the photoelastic coefficient are summarized in Table I.

It is evident from our results that the dispersion of the stress-optic fiber effect, although small, cannot be neglected when considering the performance of birefringent fibers and sensor devices. In the case of a linearly birefringent fiber, we find that the dispersive nature of the stress-optic effect contributes about 10 percent to the pulse dispersion which arises from anisotropic thermal stress within the fiber. For a circularly birefringent fiber twisted at 50 turns/m, the effect produces a pulse dispersion of ~2 ps/km.

The temperature dependence of the stress-optic coefficient is sufficient to significantly modify the temperature behavior of stress-dominated linearly birefringent fibers. It can also limit the operating temperature range of controlled-birefringence devices which are based on bend or pressure-induced birefringence, such as Faraday isolators, filters, and polarization controllers.

APPENDIX

We show that using the values for bulk silica $n_s(\lambda)$ and $dn_s/d\lambda$ in (2) and (3), instead of those for the GeO_2-doped silica fiber used in the experiment, produces a negligible error in the calculation of $C(\lambda)$ and $dC/d\lambda$.

Effect on Calculation of $C(\lambda)$

Reference to (2) reveals that

$$C(\lambda) = -\frac{n_c g'}{R} \tag{A1}$$

where n_c is the index of the fiber core. For our weakly doped fiber (relative index Δ above silica = 0.27 percent),

$$n_c = n_s(1 + \Delta). \tag{A2}$$

Thus, the error in $C(\lambda)$ is ~0.3 percent, which is negligible.

Effect on Calculation of $dC/d\lambda$

Examination of (3) indicates that the computed value of $dC/d\lambda$ depends on both $dn_c/d\lambda$ and $n_c(\lambda)$. The value of $dn_c/d\lambda$ for a fiber containing 8.1 m/o GeO_2 can be found from [31] where the variation of fiber numerical aperture (NA) with wavelength is given:

$$NA^2 = n_c^2 - n_s^2 = A + B\lambda^2 + C\lambda^{-2}. \tag{A3}$$

Differentiating, we obtain

$$\frac{dn_c}{d\lambda} = \frac{\lambda B - C\lambda^{-3}}{n_c} + \frac{n_s}{n_c}\frac{dn_s}{d\lambda}. \tag{A4}$$

Evaluating (A4) at 1.064 μm and using the silica values of n_s = 1.4496 and $dn_s/d\lambda = -1.119 \times 10^{-2}\ \mu m^{-1}$, we obtain $dn_c/d\lambda = -1.103 \times 10^{-2}\ \mu m^{-1}$ for the GeO_2-doped glass, i.e., a difference of ~1.5 percent from the value for bulk silica. The difference would be proportionally less for our fiber, which contains only 3.4 m/o GeO^2. Moreover, (3) is dominated by the second term, the term in $n_c(\lambda)$, for which we have already shown the error to be ~0.3 percent. Thus, the overall error incurred by using the values for bulk silica in (3) is ~0.3 percent.

ACKNOWLEDGMENT

We thank E. J. Tarbox, R. D. Birch, R. J. Mansfield, and M. R. Hadley for fabricating the spun fibers, I. Sasaki for the index profile, and G. W. Day and A. H. Hartog for helpful discussions.

REFERENCES

[1] V. Ramaswamy, W. G. French, and R. D. Standley, "Polarization characteristics of non-circular core single-mode fibers," *Appl. Opt.*, vol. 17, pp. 3014-3017, 1978.

[2] T. Katsuyama, H. Matsumura, and T. Suganuma, "Low-loss single-polarization fibers," *Electron. Lett.*, vol. 17, pp. 473-474, 1981.

[3] R. Ulrich and A. Simon, "Polarization optics of twisted single-mode fibers," *Appl. Opt.*, vol. 18, pp. 2241-2251, 1979.

[4] L. Jeunhomme and M. Monerie, "Polarization-maintaining single-mode fiber cable design," *Electron. Lett.*, vol. 16, pp. 921-922, 1980.

[5] S. K. Sheem and T. G. Giallorenzi, "Polarization effects on single-mode optical fiber sensors," *Appl. Phys. Lett.*, vol. 35, pp. 914-917, 1979.

[6] F. Fevre, L. Jeunhomme, I. Joindot, M. Monerie, and J. C. Simon, "Progress towards heterodyne-type single-mode fiber communication systems," *IEEE J. Quantum Electron.*, vol. QE-17, pp. 897-906, 1981.

[7] R. H. Stolen and E. H. Turner, "Faraday rotation in highly birefringent optical fibers," *Appl. Opt.*, vol. 19, pp. 842-845, 1980.

[8] G. W. Day, D. N. Payne, A. J. Barlow, and J. J. Ramskov Hansen, "Faraday rotation in coiled, monomode optical fibers: Isolators, filters and magnetic sensors," *Opt. Lett.*, vol. 7, pp. 238-240, 1982.

[9] H. C. Lefevre, "Single-mode fiber fractional wave devices and polarization controllers," *Electron. Lett.*, vol. 16, pp. 778-780, 1980.

[10] M. Johnson, "Single-mode-fiber birefringent filters," *Opt. Lett.*, vol. 5, pp. 142-144, 1980.

[11] S. C. Rashleigh, "Acoustic sensing with a single coiled monomode fiber," *Opt. Lett.*, vol. 5, pp. 392-394, 1980.

[12] P. G. Ceilo, "Fiber optic hydrophone: Improved strain configuration and environmental noise protection," *Appl. Opt.*, vol. 18, pp. 2933-2937, 1979.

[13] D. N. Payne, A. J. Barlow, and J. J. Ramskov Hansen, "Development of low- and high-birefringence optical fibers," *IEEE J. Quantum Electron.*, vol. QE-18, pp. 477-488, Apr. 1982.

[14] N. K. Sinha, "Normalized dispersion of birefringence of quartz and stress-optical coefficient of fused silica and plate glass," *Phys. Chem. Glasses*, vol. 19, pp. 69-77, 1978.

[15] I. H. Malitson, "Interspecimen comparison of the refractive index of fused silica," *J. Opt. Soc. Amer.*, vol. 55, pp. 1205-1209, 1965.

[16] N. F. Borrelli and R. A. Miller, "Determination of the individual strain-optic coefficients of glass by an ultrasonic technique," *Appl. Opt.*, vol. 7, pp. 745-750, 1968.

[17] A. J. Barlow, D. N. Payne, M. R. Hadley, and R. J. Mansfield, "Production of single-mode fibers with negligible intrinsic birefringence and polarization mode dispersion," *Electron. Lett.*, vol. 17, pp. 725-726, 1981.

[18] A. J. Barlow, J. J. Ramskov Hansen, and D. N. Payne, "Birefringence and polarization mode-dispersion in spun single-mode fibers," *Appl. Opt.*, vol. 20, pp. 2962-2968, 1981.

[19] R. Ulrich, S. C. Rashleigh, and W. Eickhoff, "Bending-induced birefringence in single-mode fibers," *Opt. Lett.*, vol. 5, pp. 273-275, 1980.

[20] C. Lin, L. G. Cohen, R. H. Stolen, G. W. Tasker, and W. G. French, "Near infrared sources in the 1-1.3 μm region by efficient stimulated Raman emission in glass fibers," *Opt. Commun.*, vol. 20, pp. 426-428, 1977.

[21] F.M.E. Sladen, D. N. Payne, and M. J. Adams, "Profile dispersion measurements for optical fibers over the wavelength range 350 nm to 1900 nm," in *Proc. 4th Euro. Conf. Opt. Commun.*, Genoa, Italy, 1978, pp. 48-57.

[22] N. Imoto, N. Yoshizawa, J. Sakai, and H. Tsuchiya, "Birefringence in single-mode optical fiber due to elliptical core deformation and stress anisotropy," *IEEE J. Quantum Electron.*, vol. QE-16, pp. 1267-1271, 1980.

[23] W. Primak and D. Post, "Photo-elastic constants of vitreous silica and its elastic coefficient of refractive index," *J. Appl. Phys.*, vol. 30, pp. 779-788, 1959.

[24] S. C. Rashleigh and R. Ulrich, "Polarization mode-dispersion in single-mode fibers," *Opt. Lett.*, vol. 3, pp. 60-62, 1978.

[25] A. J. Barlow and D. N. Payne, "Polarization maintenance in circularly birefringent fibers," *Electron. Lett.*, vol. 17, pp. 388-389, 1981.

[26] A. M. Smith, "Birefringence induced by bends and twists in single-mode optical fiber," *Appl. Opt.*, vol. 19, pp. 2606-2611, 1980.

[27] G. W. Morey, *Properties of Glass.* New York: Reinhold, 1938, pp. 430-431.

[28] S. Spinner, *J. Amer. Ceram. Soc.*, vol. 39, p. 113, 1956.

[29] G. W. Day, private communication.

[30] S. C. Rashleigh and R. Ulrich, "Magneto-optic current sensing with birefringent fibers," *Appl. Phys. Lett.*, vol. 34, pp. 768-770, 1979.

[31] M. J. Adams, *An Introduction to Optical Waveguides.* New York: Wiley, 1981, pp. 305-307.

Arthur J. Barlow was born in Banbury, England, on June 11, 1957. He received the B.Sc. degree in applied physics and electronics from the University of Durham, Durham, England, in 1978.

In 1978 he joined the Optical Communications Group, University of Southampton, Southampton, England, as a Research Student working for the Ph.D. degree on birefringence properties of single-mode fibers. Since October 1981 he has continued his studies as a Junior Research Fellow.

David N. Payne was born in Lewes, England, on August 13, 1944 and educated in Central Africa. He received the B.Sc. degree in electrical engineering, the Diploma in quantum electronics, and the Ph.D. degree from the University of Southampton, Southampton, England.

In 1972 he became the Pirelli Research Fellow in the Department of Electronics, University of Southampton, and in 1977 he was appointed to the Optical Communications Group as a Senior Research Fellow. Since 1969 his research interests have been in optical communications and have included preform and fiber fabrication techniques, optical propagation in multimode and single-mode fibers, fiber and preform characterization, wavelength-dispersive properties of optical fiber materials, optical transmission measurements, and fiber devices. Currently, his main fields of interest are polarization properties of optical fibers, fiber sensors, and optical transmission.